The Effects of Motion on Distributed Detection in Mobile Ad-Hoc Sensor Networks

Xusheng Sun and Edward J. Coyle, *Fellow*, *IEEE*

School of Electrical and Computer Engineering
Georgia Institute of Technology, Atlanta, Georgia 30332–0250
Email: {xsun7, ejc}@gatech.edu

***Abstract*— A set of mobile wireless sensors observe their environment as they move about. We consider the subset of these sensors that each made observations when they were all at approximately the same time/location. As they continue to move, one of them processes its observations and decides that an event that must be reported has taken place. To reduce the probability of a false alarm, this sensor assumes the role of a Cluster-Head (CH) and requests that all other sensors that collected observations at that time/location reply with their decisions. The motion of each sensor determines how many wireless hops its decision data must make to reach the CH. We analyze the effect of this motion in the 1D case by modeling each sensor's motion as a Correlated Random Walk (CRW), which can account for transient behavior, geographical restrictions, and nonzero drift. Quantities, such as the energy required to collect the decision from all relevant sensors and the error probability of the final decision at the CH, can then be determined as a function of time.**

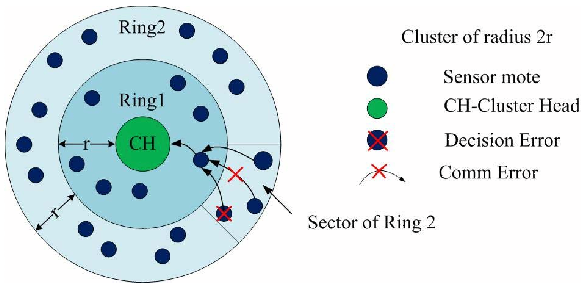

Fig. 1. A 2-hop, 2-D cluster. The mobility of the sensors produces this temporary, multi-hop cluster for applications such as detection. As they move, the cluster changes size and more hops may be required for all relevant sensors to participate. Each sensor's decision may be incorrect because of measurement noise; transmitted packets may suffer bit errors because of noisy communication channels. If the number of hops in the cluster increases with time, the energy required for communication will increase and detection performance will decrease.

I. Introduction

In an ad-hoc mobile wireless sensor network, mobile sensors sample their environment, process these samples to make local decisions, and transmit/relay these decisions as needed. We consider a group of sensors that have each collected a sample in a specified spatial region and time interval. They process their samples as they continue to move. The first sensor to get a positive result floods the network with a request for decisions from all others that took samples within the same spatiotemporal region. These other sensors report back to the requesting sensor, which is called the Cluster Head (CH) [1]. The CH fuses these decisions with its own to obtain a more reliable decision [2].

In the 2D case, the communication architecture for this application looks like the 2-hop cluster shown in Fig. 1. The sensor in the center of the cluster, the CH, is the one that requested the decisions from other sensors. The sensors shown in the first ring are one wireless hop from the CH; the ones in the second ring are two hops away. Three sensors in a sector of ring 2 are shown forwarding their decisions to one sensor in ring 1. Each sensor's observation is affected by measurement noise and all communications throughout the network will be affected by channel noise, fading, and transceiver errors. Because the cluster is multi-hop, decisions forwarded from the outer rings will suffer repeated exposure to the sources of communication error and more energy must expended to get them to the CH. The mobility model governing each sensor will therefore affect the number of hops, and thus the detection accuracy at the CH and the energy consumed to achieve this level of accuracy. It will also affect the network's performance in terms of coverage, maximum throughput, and throughput-delay trade-offs.

Many mobility models have been proposed for analyzing the behavior of mobile ad hoc networks. In [3], [4], those models are categorized into four classes: random models, models with temporal dependency, models with spatial dependency, and models with geographic restrictions. For instance, random walks and random waypoint models are random models; Gauss-Markov mobility models and Smooth Random models are models with temporal dependency; group mobility models [3] are models with spatial dependency; Pathway mobility models and Obstacle mobility models are models with geographic restrictions. These models are all useful as analytical or simulation tools but none of them can account for all the constraints in real systems.

Correlated Random Walks (CRWs) have thus been proposed as a mobility model that accounts for time dependency, geographical restrictions and nonzero drift. They are more general than random walks but still easy to analyze. The limiting distributions for a discrete-time 1-D completely infinite CRW is derived in [5]. The probabilities of being at any lattice point at the nth step for a discrete-time 1-D CRW in different cases

are solved in [6]–[9]. The absorbing probability and expected duration of a discrete-time CRW is solved in [10]. For the transient behavior of the continuous-time CRW, the semi-infinte 1-D case is solved in [11]. The behavior of multiple sensors whose motion is modeled by processes related to CRWs is studied in [12]. In this paper, we focus on continuous-time 1-D CRWs on finite state-spaces.

This paper is organized as follows. In section II, the transient behavior of semi-infinite correlated random walks is reviewed. The solution to the finite case, which is a good model for the motion of vehicles or people in a sector of a city, is provided in section III. Its statistical properties are analyzed in section IV. In section V, the detection problem in mobile wireless sensor networks is studied. Numerical results are shown in section VI. They demonstrate: (i) the use of the mobility model to determine the energy required to collect data from each participating sensor; (ii) the error probability at the cluster head once the decisions from all participating sensors have been gathered. Both the energy required and the error probability are functions of time and the parameters of the mobility model. Some conclusions and a discussion of future work are provided in Section VI.

II. Transient Analysis of a Correlated Random Walk on $[0, \infty)$

In this section, we briefly review results on the transient probability distributions of a continuous-time 1D CRW on $[0, \infty)$ [11]. In this case, the sensor moves according to the following rules:

It takes a step in the same direction as its previous step with probability p_1 or p_2 depending on whether its previous step was in the positive or negative direction, respectively. It takes a step in the opposite direction of its previous step with probability $q_1 = 1 - p_1$ or $q_2 = 1 - p_2$ depending on whether its previous step was in the positive or negative direction, respectively. On reaching a (reflecting) boundary, it takes a step in the opposite direction with probability one.

The time at which it takes its next step is governed by a Poisson process of intensity λ.

A CRW on $[0, \infty)$ with a reflecting boundary at 0 can be modeled as a quasi-birth-death (QBD) process with the state transition diagram shown in Fig. 2. The state $n-$ at any level n is entered when the sensor moves to location n from location $n + 1$. The state $n+$ any level n is entered when the sensor moves to location n from location $n - 1$.

Letting Q denote the generator for this QBD process, the Laplace transform $\Pi(s)$ of the vector $\pi(t)$ of transient probabilities for all states in the process satisfies the equations: [13]

$$\Pi(s)(Q - sI) = -\pi(0), \pi(0) = \pi(t)|_{t=0} \tag{1}$$

For this QBD process,

$$Q = \begin{bmatrix} -\lambda & \lambda & 0 & 0 & 0 & 0 & 0 & 0 & \dots \\ q_1\lambda & -\lambda & 0 & p_1\lambda & 0 & 0 & 0 & 0 & \dots \\ p_2\lambda & 0 & -\lambda & q_2\lambda & 0 & 0 & 0 & 0 & \dots \\ 0 & 0 & q_1\lambda & -\lambda & 0 & p_1\lambda & 0 & 0 & \dots \\ 0 & 0 & p_2\lambda & 0 & -\lambda & q_2\lambda & 0 & 0 & \dots \\ 0 & 0 & 0 & 0 & q_1\lambda & -\lambda & 0 & p_1\lambda & \dots \\ 0 & 0 & 0 & 0 & p_2\lambda & 0 & -\lambda & q_2\lambda & \dots \\ \vdots & \vdots & \vdots & \vdots & \vdots & \vdots & \ddots & & \end{bmatrix} \tag{2}$$

For simplicity only, assume the initial position of the sensor is 0; i.e., $\pi(0) = [1, 0, 0, \cdots]$. Define $\Pi_n(s)$ to be the transform of $\pi_n(t)$, the vector of transient probabilities for states on level n of the process.

$$-(\lambda + s)\Pi_0(s) + \Pi_1(s) \begin{bmatrix} q_1\lambda \\ p_2\lambda \end{bmatrix} = -1, \tag{3}$$

$$\lambda\Pi_0(s) + \Pi_1(s) \begin{bmatrix} -(\lambda + s) \\ 0 \end{bmatrix} = 0, \tag{4}$$

$$\Pi_n(s)B(s) + \Pi_{n+1}(s)C(s) = 0, n \geq 1, \tag{5}$$

where

$$B(s) = \begin{bmatrix} 0 & p_1\lambda \\ -(\lambda + s) & q_2\lambda \end{bmatrix} \tag{6}$$

$$C(s) = \begin{bmatrix} q_1\lambda & -(\lambda + s) \\ p_2\lambda & 0 \end{bmatrix} \tag{7}$$

Thus we get

$$\Pi_{n+1}(s) = \Pi_n(s)W(s), \tag{8}$$

where

$$W(s) = -B(s)[C(s)]^{-1} = \begin{bmatrix} \frac{p_1\lambda}{\lambda+s} & -\frac{p_1q_1\lambda}{p_2(\lambda+s)} \\ \frac{q_2\lambda}{\lambda+s} & \frac{\lambda+s}{p_2\lambda} - \frac{q_1q_2\lambda}{p_2(\lambda+s)} \end{bmatrix}. \tag{9}$$

The boundary variables must satisfy the following equation:

$$\Pi_1(s)p_1(s) = 0. \tag{10}$$

where $p_1(s)$ denotes the right eigenvector corresponding to the eigenvalue of $W(s)$ whose magnitude is greater than or equal to 1 for all possible values of s. For this CRW, $W(s)$ is diagonalizable and its eigenvalues are given by:

$$\lambda_k(s) = \frac{f(s) - (-1)^k\sqrt{(f(s))^2 - 4p_1p_2\lambda^2(\lambda + s)^2}}{2p_2\lambda(\lambda + s)} \tag{11}$$

where $f(s) = (p_1 + p_2)\lambda^2 + 2s\lambda + s^2$, for $k = 1, 2$. The right eigenvectors $p_k(s)$, $k = 1, 2$ corresponding to the eigenvalues $\lambda_1(s)$ and $\lambda_2(s)$ are given by

$$p_k(s) = \begin{bmatrix} \frac{f(s)-2p_1p_2\lambda^2+(-1)^k\sqrt{(f(s))^2-4p_1p_2\lambda^2(\lambda+s)^2}}{2p_2(p_2-1)\lambda^2} \\ 1 \end{bmatrix}. \tag{12}$$

We find numerically that, for all possible values of p_1, p_2, λ, and s, the magnitude of $\lambda_1(s)$ is greater than or equal to 1.

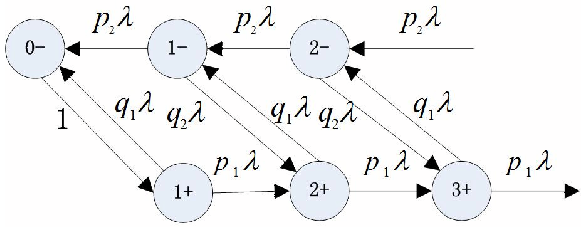

Fig. 2. A Correlated Random Walk (CRW) on $[0, \infty)$.

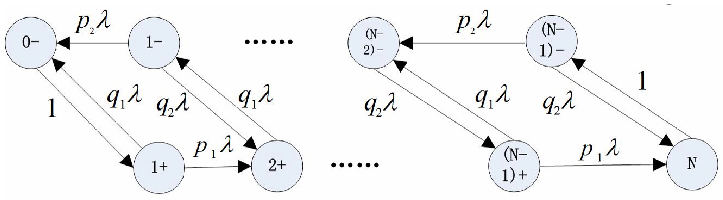

Fig. 3. a Correlated Random Walk on $[0, N]$.

Hence,

$$\Pi_{1+}(s) = \frac{2\lambda(1-p_2)}{(p_1+p_2-1)\lambda^2 + (1-2p_2)(s+\lambda)^2 + g(s)} \tag{13}$$

where $g(s) =$

$$\sqrt{(s+\lambda)^4 - [(1-2p_1)(1-2p_2)+1]\lambda^2(\lambda+s)^2 + (p_1+p_2-1)^2\lambda^4} \tag{14}$$

III. Transient Analysis of a Correlated Random Walk on $[0, N]$

A CRW on $[0, N]$ with reflecting boundaries at 0 and N can be modeled as a QBD process with the state transition diagram shown in Fig. 3 and the following generator:

$$Q = \begin{bmatrix} -\lambda & \lambda & 0 & 0 & 0 & 0 & \dots & 0 & 0 \\ q_1\lambda & -\lambda & 0 & p_1\lambda & 0 & 0 & \dots & 0 & 0 \\ p_2\lambda & 0 & -\lambda & q_2\lambda & 0 & 0 & \dots & 0 & 0 \\ 0 & 0 & q_1\lambda & -\lambda & 0 & p_1\lambda & \dots & 0 & 0 \\ 0 & 0 & p_2\lambda & 0 & -\lambda & q_2\lambda & \dots & 0 & 0 \\ \vdots & \vdots & \vdots & \vdots & \vdots & \vdots & \ddots & \vdots & \vdots \\ 0 & 0 & 0 & 0 & \dots & q_1\lambda & -\lambda & 0 & p_1\lambda \\ 0 & 0 & 0 & 0 & \dots & p_2\lambda & 0 & -\lambda & q_2\lambda \\ 0 & 0 & 0 & 0 & \dots & 0 & 0 & \lambda & -\lambda \end{bmatrix} \tag{15}$$

We assume w.l.o.g. that the initial position of the sensor is 0; i.e., $\pi(0) = [1, 0, \dots, 0]$. Then we get

$$-(\lambda+s)\Pi_0(s) + \Pi_1(s)\begin{bmatrix} q_1\lambda \\ p_2\lambda \end{bmatrix} = -1, \tag{16}$$

$$\lambda\Pi_0(s) + \Pi_1(s)\begin{bmatrix} -(\lambda+s) \\ 0 \end{bmatrix} = 0, \tag{17}$$

$$\lambda\Pi_N(s) + \Pi_{N-1}(s)\begin{bmatrix} 0 \\ -(\lambda+s) \end{bmatrix} = 0, \tag{18}$$

$$-(\lambda+s)\Pi_N(s) + \Pi_{N-1}(s)\begin{bmatrix} p_1\lambda \\ q_2\lambda \end{bmatrix} = 0, \tag{19}$$

$$\Pi_n(s)B(s) + \Pi_{n+1}(s)C(s) = 0, 1 \le n \le N-2. \tag{20}$$

IV. Statistical Properties

For the CRW on $[0, N]$, the steady state probability of being at any location n is [9]:

$$\begin{aligned} \bar{\pi}_0 &= \frac{1}{2}\frac{(p_1/p_2)-1}{(p_1/p_2)^N - 1}, \\ \bar{\pi}_N &= \bar{\pi}_0(p_1/p_2)^{N-1}, \\ \bar{\pi}_n &= \bar{\pi}_0(1+p_1/p_2)(p_1/p_2)^{N-1}, n = 1, 2, \dots, (N-1). \end{aligned} \tag{21}$$

For the special case of $p_1 = p_2 = p$,$\bar{\pi}_0 = \bar{\pi}_N = 1/(2N)$ and $\bar{\pi}_n = 1/N, 1, 2, \dots, (N-1)$.

Suppose the CH is static and there are a total of K sensors in the cluster. They start at the the same location as the CH and move independently based on identical but independent CRW models. Define $x_i(t)$ as the location of the ith sensor at time t. Further define $d_{\max}(t)$ and $d_{\min}(t)$ as the maximum distance and the minimum distance between any sensor in the cluster and the CH, respectively. Then,

$$\begin{aligned} P(d_{\max}(t) = n) &= P(d_{\max}(t) \le n) - P(d_{\max}(t) \le n-1) \\ &= P(x_1(t) \le n)^K - P(x_1(t) \le n-1)^K \\ &= (\sum_{l=0}^{n} \pi_l(t))^K - (\sum_{l=0}^{n-1} \pi_l(t))^K \end{aligned} \tag{22}$$

and

$$\begin{aligned} P(d_{\min}(t) = n) &= P(d_{\min}(t) \ge n) - P(d_{\min}(t) \ge n+1) \\ &= P(x_1(t) \ge n)^K - P(x_1(t) \ge n+1)^K \\ &= (\sum_{l=n}^{N} \pi_l(t))^K - (\sum_{l=n+1}^{N} \pi_l(t))^K \end{aligned} \tag{23}$$

If the CH is also mobile and its position is governed by a CRW, then $d_{\max}(t)$ and $d_{\min}(t)$ become the maximum distance and the minimum distance between a specified sensor and any other sensor in the cluster. The probabilities remain the same whether the sensor is designated as the CH before or after motion of the sensors begins. Denote the position of the CH by $x_0(t)$. We have

$$\begin{aligned} &P\left(d_{\max}(t) = n\right) \\ &= \sum_{m=0}^{N} P(x_0(t) = m) P(d_{\max}(t) = n | x_0 = m) \end{aligned} \tag{24}$$

$$
\begin{aligned}
&= \sum_{m=0}^{N} P(x_0(t)=m)[P(d_{\max}(t) \le n | x_0 = m) \\
&\quad - P(d_{\max}(t) \le n-1 | x_0 = m)] \\
&= \sum_{m=0}^{N} P(x_0(t)=m)[P(m-n \le x_i(t) \le m+n, 1 \le i \le K) \\
&\quad - P(m-n+1 \le x_i(t) \le m+n-1, 1 \le i \le K)] \\
&= \sum_{m=0}^{N} \pi_m(t) \left[\left(\sum_{l=m-n}^{m+n} \pi_l(t) \right)^K - \left(\sum_{l=m-n+1}^{m+n-1} \pi_l(t) \right)^K \right] \\
&P\left(d_{\min}(t)=n\right) \qquad (25) \\
&= \sum_{m=0}^{N} P(x_0(t)=m)[P(d_{\min}(t) \ge n | x_0 = m) \\
&\quad - P(d_{\min}(t) \ge n+1 | x_0 = m)] \\
&= \sum_{m=0}^{N} \pi_m(t) \left(\sum_{l=0}^{m-n} \pi_l(t) + \sum_{l=m+n}^{N} \pi_l(t) \right)^K \\
&\quad - \sum_{m=0}^{N} \pi_m(t) \left(\sum_{l=0}^{m-n-1} \pi_l(t) + \sum_{l=m+n+1}^{N} \pi_l(t) \right)^K
\end{aligned}
$$

The probability distribution of the distance between any two sensors $d(t)$ is:

$$P(d(t)=0) = \sum_{m=0}^{N} \pi_m(t)^2 \qquad (26)$$

and for $n \neq 0$,

$$P(d(t)=n) = \sum_{m=0}^{N} \pi_m(t)(\pi_{m+n}(t) + \pi_{m-n}(t)) \qquad (27)$$

Define $D_{\max}(t)$ and $D_{\min}(t)$ as the maximum distance and the minimum distance between any two sensors in the cluster. Then,

$$
\begin{aligned}
&P\left(D_{\max}(t)=0\right) \\
&\quad = \sum_{m=0}^{N} P(x_i(t)=m, 1 \le i \le K) = \sum_{m=0}^{N} \pi_m(t)^K \qquad (28)
\end{aligned}
$$

and for $n \neq 0$,

$$
\begin{aligned}
&P\left(D_{\max}(t)=n\right) \qquad (29) \\
&= \sum_{m=0}^{N-n} P(\min\{x_i(t)\} = m \bigcap \\
&\quad \max\{x_i(t)\} = m+n, 1 \le i \le K) \\
&= \sum_{m=0}^{N-n} \sum_{l=1}^{K-1} \sum_{r=1}^{K-l} \binom{K}{l} \binom{K-l}{r} \pi_m(t)^l \pi_{m+n}(t)^r \\
&\quad \left(\sum_{s=m+1}^{m+n-1} \pi_s(t) \right)^{K-l-r}
\end{aligned}
$$

where l sensors are at the location m and r sensors are at the location $m+n$, while all the others are in between. The calculation of the probability distribution of $D_{\min}(t)$ is much more complicated and, when $K > N$, it is always zero.

V. Detection in Wireless Sensor Networks

This paper assumes a multi-hop sensor network in which each wireless hop is modeled as a Binary Symmetric Channel (BSC). The BSC cross-over probability captures the effect of channel errors on each individual decision bit and is easier to estimate than the full characteristics of the channel. The assumptions of symmetry and the same cross-over probability for each mote-to-mote channel are easily relaxed – they are used only to simplify the analysis so that important trends can be discerned. This paper also assumes that the error probabilities of the individual received detection results are learned over time by the CH. Hence, the CH is assumed to know the optimal weights for the weighted median in the MAP detector [14] it uses to fuse the received detection results.

In [14], a MAP approach to the distributed detection problem in a multi-hop cluster in a sensor network was developed. It considered a cluster with K rings and N_k motes in the kth ring. Each mote makes a decision between two hypotheses, $s_0 = 0$ and $s_1 = 1$, where "1" denotes that an event has occurred and "0" that it has not. The detection results by different motes are assumed to be i.i.d. Bernoulli random variables, each with a detection error probability $p_m < 1/2$. The noise processes in different wireless channels are assumed to be independent and white. Each hop in the network is modeled as a BSC with cross-over probability $p_c < 1/2$. The decisions made by motes in the outer rings are relayed by the motes in inner rings to the CH. Let the error probability of the detection results received by the CH from the kth ring be $p_{e,k}$. Then, for example, $p_{e,1} = p_c(1-p_m)+p_m(1-p_c)$. Denote the detection result received by the CH from the ith mote in the kth ring by $r_{k,i}$ and arrange the detection results in the same ring in a vector $\bar{r}_k = (r_{k,1}, r_{k,2}, \ldots, r_{k,N_k}), k = 1, 2, \ldots, K$. Let E denote the event that a decision error happens at the CH.

In a *one*-hop cluster, suppose the correct decision should be s. Assume the prior probability $p(s = s_0) = p < 1/2$ and find a real number χ such that $\ln((1-p)/p) = \chi \ln((1-p_{e,1})/p_{e,1})$. Define $W = \lfloor N_1/2 + \chi/2 \rfloor$. The MAP-based decision bit at the CH is $\hat{r} = (\bar{r}_1)_W = W$'th order statistic of $(r_1, r_2, \ldots, r_{N_1})$. The decision error probability at the CH is:

$$
\begin{aligned}
P(E) = (1-p) &\left(\sum_{i=W}^{N_1} \binom{N_1}{i} (p_{e,1})^i (1-p_{e,1})^{N_1-i} \right) \\
&+ p \left(\sum_{i=N_1-W}^{N_1} \binom{N_1}{i} (p_{e,1})^i (1-p_{e,1})^{N_1-i} \right) \qquad (30)
\end{aligned}
$$

It is shown in [14] that, as an estimate of the true decision bit, this weighted order statistic is biased but asymptotically unbiased. When the prior probability is $p = 1/2$, it simplifies into a binary median filter.

Now we summarize key results in [14] for the *multi*-hop case. For a mote that is k hops away from the CH, the detection result received by the CH after being relayed over these hops

has error probability:

$$p_{e,k} = \frac{1}{2} - \frac{1}{2}(1-2p_m)(1-2p_c)^k, k \geq 1 \quad (31)$$

We use the notation $W \diamondsuit x$, which means x should be duplicated W times. For simplicity, suppose the prior probabilities are $p(s = s_0) = p(s = s_1) = 1/2$.

Theorem 1: Define $\chi_k = \ln((1-p_{e,k})/p_{e,k})$, and assume these χ_k's can be scaled so that $\chi_1 : \chi_2 : \ldots : \chi_K = W_1 : W_2 : \ldots : W_K$, where the W_k's are positive integers with $gcd(W_1, W_2, \ldots, W_K) = 1$. The MAP-based decision bit is then given by $\hat{r} = Median(W_1 \diamondsuit \bar{r}_1, W_2 \diamondsuit \bar{r}_2, \ldots, W_K \diamondsuit \bar{r}_K)$. The decision error probability at the CH is given by:

$$P(E) = \sum_{\sum W_k(2c_k - N_k) > 0} \prod_{k=1}^{K} \binom{N_k}{c_k} (p_{e,k})^{c_k} (1-p_{e,k})^{N_k - c_k} \quad (32)$$

where c_k is the number of occurrences of $1-s$ in the vector $\bar{r}_k, k = 1, 2, \ldots, K$.

■

Because the weighted median is the MAP detector, we assume – even for sector-level fusion algorithms – that the CH calculates this weighted median after receiving inputs from all motes in the cluster. To understand what happens in these more complex cases, the asymptotic behavior of the weighted median must be determined for the single- *and* multi-hop cases; otherwise, it is too difficult to determine the probability of a cluster-wide decision error at the CH.

The asymptotic behavior of the median filter in one-hop clusters has thus been studied using large deviation techniques in [15]:

$$\lim_{N_1 \to \infty} -\frac{1}{N_1} P(E) = C(p_{e,1})$$
$$C(p_{e,1}) = -\ln(2) - \frac{1}{2}\ln(p_{e,1}(1-p_{e,1})) \quad (33)$$

We now find the error exponent for the decision error probability for the multi-hop case.

Theorem 2: In multi-hop sensor networks in which $p_{e,k}$ is the error probability of the individual detection results received by the CH from nodes in ring k, the error probability of the MAP detector is upper bounded by: [16]

$$\ln(P(E)) \leq \sum_{k=1}^{K} N_k [\ln(2) + \frac{1}{2}\ln(p_{e,k}(1-p_{e,k}))] \quad (34)$$

Proof: In the context of the weighted median filter, the decision error probability at the CH is:

$$P(E) = P(\sum_{k=1}^{K} W_k \sum_{i=1}^{N_k} r_{k,i} \geq \sum_{k=1}^{K} W_k N_k/2)$$
$$= P(\sum_{k=1}^{K} \sum_{i=1}^{N_k} W_k (r_{k,i} - 1/2) \geq 0) \quad (35)$$

Since $P(Z \geq 0) \leq E[e^{Zt}]$, let $r'_{k,i} = r_{k,i} - 1/2$, and $E[r'_{k,i}] = p_{e,k} - 1/2 < 0$. We have:

$$P(E) \leq E[e^{t\sum_{k=1}^{K}\sum_{i=1}^{N_k} W_k r'_{k,i}}] = \prod_{k=1}^{K}\prod_{i=1}^{N_k} E[e^{tW_k r'_{k,i}}]$$

For each term in the product, $E[e^{tW_k r'_{k,i}}] = p_{e,k}e^{\frac{1}{2}tW_k} + (1-p_{e,k})e^{-\frac{1}{2}tW_k}$. Setting $\frac{\partial E[e^{tW_k r'_{k,i}}]}{\partial t} = 0$, we find:

$$\frac{1}{2}W_k p_{e,k} e^{\frac{1}{2}tW_k} = \frac{1}{2}W_k(1-p_{e,k})e^{-\frac{1}{2}tW_k}$$
$$t = 1 \quad (36)$$

■

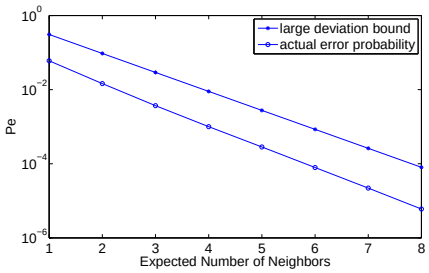

Fig. 4. Comparison for a 3-ring cluster of the error probability obtained via simulation and its large deviations bound. The error exponent is clearly correct and the difference approaches zero asymptotically. Comparing the performance of complex strategies via their error exponents will thus correctly show which strategy is best when motes have large numbers of 1-hop neighbors. Direct calculations and simulations are used to confirm those results for small to moderate numbers of neighbors.

This error exponent is accurate and the bound is tight when the motes are densely deployed; i.e., the number of sensors is large. Minimizing $P(E)$ when the number of motes is finite is a very difficult combinatorial problem, so we can minimize this upper bound instead. Also note that the effect of each ring of motes on the decision error probability at the CH is apparent in this bound. It may thus be used to simplify many optimization problems in distributed detection in multi-hop scenarios.

Fig.4 compares the large deviation bound on the error probability with the error probability from simulations for a 3-ring cluster. It shows the desired result that the large deviation error exponent is accurate – the bound is parallel with the simulation result over the entire range of spatial densities. Of course, the bound is high by a multiplicative factor, which is often the case with large deviation techniques.

If the CH is static, then we have

$$P(E) \leq E\left[\prod_{i=1}^{K} 2\sqrt{p_{e,i}(1-p_{e,i})}\right]$$
$$= \prod_{i=1}^{K} E\left[2\sqrt{p_{e,i}(1-p_{e,i})}\right]$$
$$= \left[E\left[2\sqrt{p_{e,1}(1-p_{e,1})}\right]\right]^K \quad (37)$$

where

$$p_{e,1} = \frac{1}{2} - \frac{1}{2}(1-2p_m)(1-2p_c)^{\lceil x_1(t)/r \rceil} \quad (38)$$

The expected energy consumption for collecting the data is then

$$C = K\lceil E[x_1(t)]/r \rceil \quad (39)$$

If the CH is also mobile and its position is governed by a CRW, then we have

$$\begin{aligned} P(E) &\leq \sum_{m=0}^{N} P(x_0(t)=m)P(E|x_0(t)=m) \quad (40)\\ &= \sum_{m=0}^{N} P(x_0(t)=m) \prod_{i=1}^{K} E\left[2\sqrt{p_{e,i}(1-p_{e,i})}|x_0(t)=m\right] \\ &= \sum_{m=0}^{N} P(x_0(t)=m) \left[E\left[2\sqrt{p_{e,1}(1-p_{e,1})}|x_0(t)=m\right]\right]^K \end{aligned}$$

where

$$p_{e,1} = \frac{1}{2} - \frac{1}{2}(1-2p_m)(1-2p_c)^{\lceil d(t)/r \rceil} \quad (41)$$

The expected energy consumption for collection of the data is

$$C = K\lceil E[d(t)]/r \rceil \quad (42)$$

VI. Numerical Results

Fig. 5 shows the transient probability distribution of two CRWs on [0,10] with different parameters. One CRW is asymmetric, which means the walker tends, in the case shown, to prefer motion to the right. The other CRW is asymmetric, which means that the walker has no preference for one direction or the other – but its motion is still correlated.

Fig. 6 shows the transient probability distribution of the distance from a static clusterhead to the furthest of five mobile sensors for each point in time. The static clusterhead is assumed to be at location 0. This distance d is important for calculating the number of wireless hops between each sensor and the CH that is trying to gather data. If the transmission radius of each sensor is r, then the number of hops to the CH is the ceiling of d/r.

Fig.7 shows the transient probability distribution of the maximum distance between any of the five sensors and the CH when the mobile CH moves according to the same mobility model as the sensors. This is probably the most realistic case for mobile networks. It leads to an interesting phenomenon when the motion is on a finite grid and the CRWs are all asymmetric in the same direction. The sensors start at 0 when they gathered their observations. With time, they spread out but all tend to move to the right. As they get close to the other barrier, they then tend to bunch up again. This effect is similar to a crowd moving in a given direction and then gathering around that destination. The distance here, when divided by the transmission radius of the sensors tells the maximum size, in wireless hops, of the cluster.

Fig. 8 shows the expected energy consumed – as a function of the time at which data collection starts – for a static or mobile CH to collect one packet of data from five mobile sensors. The six sensors all collected measurements at the same time/place but then continued to move. By the time a request to send in all data has been received, they are at locations in the state space with probabilities determined by their CRWs. The data collected and decisions made by the sensors that have wandered the furthest require the most energy to collect – that data must travel over the largest number of hops to reach the CH.

Also note that the mobility of the CH has a significant impact on the energy consumed to collect data. If it is mobile and all sensors are moving according to a CRW that is asymmetric, then the energy required for collection first increases and then decreases. In this case, it is better to collect data either very quickly after the event, or, if that is not possible because of the time to process measurements, to wait until the CH and the other sensors bunch up again at their destination.

Fig. 9 shows the large deviation bound of the error probability as a function of time for a static or mobile CH to collect one packet of data from five mobile sensors. It shows good agreement with the results in Fig.8, which shows the expected energy consumption as a function of time for a static or mobile CH to collect one packet of data from five mobile sensors.

Fig. 10 shows the expected error probability as a function of time for a static or mobile CH to collect one packet of data from five mobile sensors. The same comments made previously about the effects of the mobility of the clusterhead, and the effects of symmetric and asymmetric walks, apply here.

VII. Conclusions

In this paper, the solution to the finite state space CRW was provided and its statistical behavior was studied both analytically and numerically. As an illustration of the application-specific performance measures it can help address, we studied the impact of motion on the energy required to gather decisions from each sensor in a multi-hop cluster created by the mobility of these sensors and the error probability of the final decision made based on those individual ones. In [17], we have given a thorough solution to the problem of distributed estimation in multi-hop wireless sensor networks. In future research, we will study the impact of motion on the energy required to gather data and the variance of the final estimate in complex mobile wireless sensor networks.

References

[1] S. Bandyopadhyay, Q. Tian and E.J. Coyle, "Spatio-temporal sampling rates and energy efficiency in wireless sensor networks," *IEEE/ACM Trans. Netw.*, vol. 13, no. 6, pp. 1339–1352, Dec. 2005.

[2] S. Bandyopadhyay and E.J. Coyle, "Minimizing communication costs in hierarchically clustered networks of wireless sensors," *Comput. Netw.*, vol. 44, no. 1, pp. 1–16, Jan. 2004.

[3] F. Bai and A. Helmy, "A survey of mobility modeling and analysis in wireless ad hoc networks," *Wireless Ad Hoc and Sensor Networks*, Kluwer Academic Publishers, Jun. 2004.

[4] T. Camp, J. Boleng, and V. Davies, "A survey of mobility models for ad hoc network research," *Wireless Commun. and Mobile Computing*, special issue on mobile and ad hoc networking: research, trends, and applications,vol.2, no.5, pp.483-502,2002.

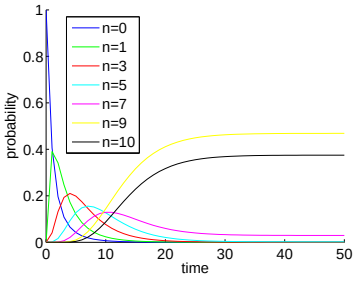

(a) An asymmetric CRW with p_1=0.8, p_2=0.2. The walker starts at 0 and then drifts toward and tends to stay near 10.

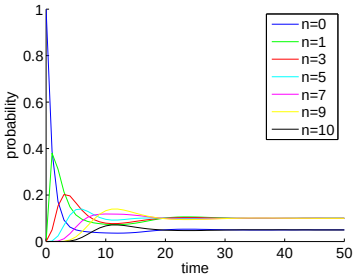

(b) A symmetric CRW with p_1=0.9, p_2=0.9. The walker starts at 0 and then it is eventually equally likely to be in each position except a boundary state.

Fig. 5. Transient probability distribution of two CRWs on [0,10]. The curve for a given *n* shows the probability that the walker is at position *n* at time t.

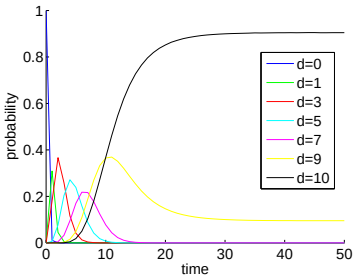

(a) All sensors move according to asymmetric CRWs with p_1=0.8, p_2=0.2

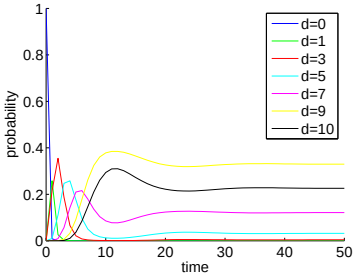

(b) All sensors move according to symmetric CRWs with p_1=0.9, p_2=0.9

Fig. 6. Transient probability distribution of the distance from a static CH to the furthest of five sensors that are moving according to independent CRWs on [0,10].

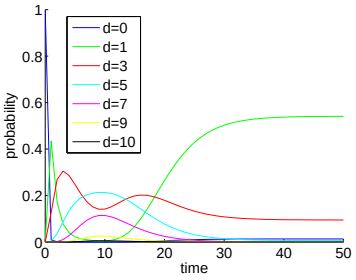

(a) All sensors move according to asymmetric CRWs with p_1=0.8, p_2=0.2

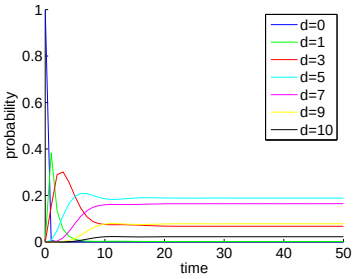

(b) All sensors move according to symmetric CRWs with p_1=0.9, p_2=0.9

Fig. 7. Transient probability distribution of the distance from a mobile CH to the furthest of five sensors. The CH and the sensors are all moving independently and according to CRWs on [0,10].

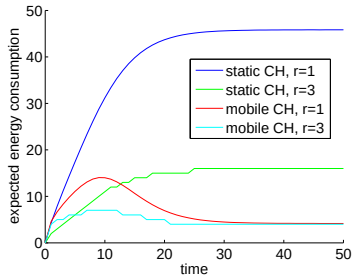

(a) All sensors move according to asymmetric CRWs with p_1=0.8, p_2=0.2

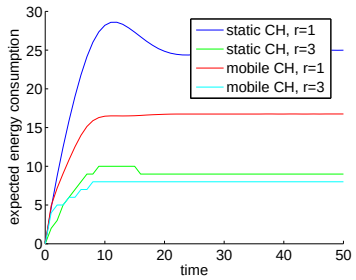

(b) All sensors move according to symmetric CRWs with p_1=0.9, p_2=0.9

Fig. 8. Expected energy consumed by the network when the collection of data from the five mobile sensors begins at time t. The cases considered are when the transmission radius of each sensor is *r=1* or *r=3* and all sensors move according to symmetric or asymmetric CRWs.

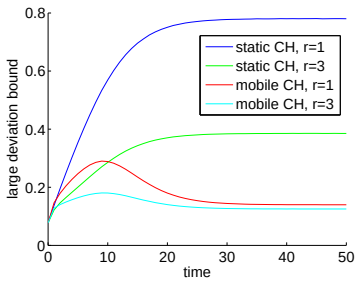

(a) All sensors move according to asymmetric CRWs with p_1=0.8, p_2=0.2

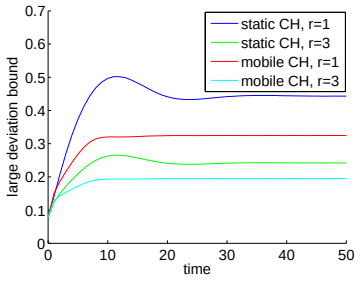

(b) All sensors move according to symmetric CRWs with p_1=0.9, p_2=0.9

Fig. 9. Large deviation bound of the error probability when the collection of data from the five mobile sensors begins at time t. The cases considered are when the transmission radius of each sensor is *r=1* or *r=3* with $p_m = 0.10$ and $p_c = 0.05$ and all sensors move according to symmetric or asymmetric CRWs.

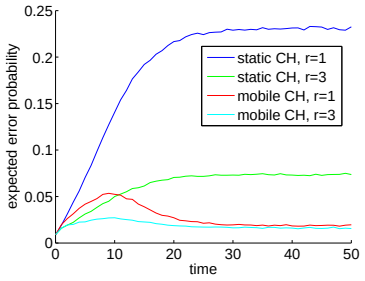

(a) All sensors move according to asymmetric CRWs with p_1=0.8, p_2=0.2

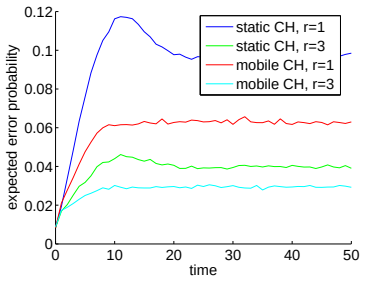

(b) All sensors move according to symmetric CRWs with p_1=0.9, p_2=0.9

Fig. 10. Expected error probability when the collection of data from the five mobile sensors begins at time t. The cases considered are when the transmission radius of each sensor is *r=1* or *r=3* with $p_m = 0.10$ and $p_c = 0.05$ and all sensors move according to symmetric or asymmetric CRWs.

[5] S. Goldstain, "On diffusion by discontinuous movements, and on telegraph equation," *Quarterly J. Mechanics and Applied Math.*, vol. 4, pp. 129–156, 1951.

[6] E. Renshawn and R. Henderson , "The correlated random walk," *J. Applied Probability.*, vol. 18, pp. 403–414, 1981.

[7] W. Bohm, "The correlated random walk with boundaries: a combinatorial solution," *J. Applied Probability.*, vol. 37, pp. 470–479, 2000.

[8] A. D. Proudfoot and D. G. Lampard, "A random walk problem with correlation," *J. Applied Probability.*, vol. 9, pp. 436–440, 1972.

[9] R. Lal and U.N.Bhat, "Some explicit results for correlated random walk," *J. Applied Probability.*, vol. 27, pp. 757–766, 1989.

[10] Y. L. Zhang, "Some problems on a one-dimensonal correlated random walk with various types of barriers," *J. Applied Probability.*, vol. 29, pp. 196–201, 1992.

[11] S. Bandyopadhyay and E. J. Coyle, "Stochastic properties of mobility models in mobile ad hoc networks," *IEEE Trans. Mobile Computing*, vol. 6, no. 11, pp. 1218–1229, Nov. 2007.

[12] H. Cai and D.-Y. Eun, "Toward Stochastic Anatomy of Inter-meeting Time Distribution under General Mobility Models," *ACM MobiHoc*, Hong Kong, May, 2008.

[13] J. Zhang and E. J. Coyle, "Transient analysis of quasi-birth-death processes," *Comm.Statistics Stochastic Models*, vol. 5, pp. 459–496, 1989.

[14] Q. Tian and E. J. Coyle, "Optimal distributed detection in clustered wireless sensor networks," *IEEE Trans. Signal Processing*, vol. 55, no. 7, pp. 3892–3904, Jul. 2007.

[15] J. -F. Chamberland and V. V. Veeravalli, "Asymptotic results for decentralized detection in power constrained wireless sensor networks," *IEEE J. Sel. Areas Communications*, vol. 22, no. 6, pp. 1007–1015, Aug. 2004.

[16] X. Sun and E. J. Coyle, "Low-complexity algorithms for event detection in wireless sensor networks," conditionally accepted by*IEEE J. Sel. Areas. Commun.*, 2009.

[17] X. Sun and E.J. Coyle, "Quantization, Channel Compensation, and Energy Allocation for Estimation in Wireless Sensor Networks," in *7'th Intl. Symposium on Modeling and Optimization in Mobile, Ad Hoc, and Wireless Networks (WiOpt 2009)*, June 23-27, 2009.